Chemical Engineering Journal 105 (2004) 1–10

Chemical Engineering Journal

www.elsevier.com/locate/cej

Kinetics of oxidation of hydroquinone by polymer-supported hypervalent iodine oxidant, iodoxybenzoic acid

S. Jegasothy[a], N.K.H. Slater[a,*], C. Denecker[b], D.C. Sherrington[b], Z. Lei[c], A.J. Sutherland[c]

[a] *Department of Chemical Engineering, University of Cambridge, New Museums Site, Pembroke Street, Cambridge CB23RA, UK*

[b] *Department of Pure and Applied Chemistry, University of Strathclyde, Glasgow, UK*

[c] *Chemical Engineering and Applied Chemistry, Aston University, Birmingham, UK*

Received 28 September 2004; accepted 28 September 2004

Abstract

Iodoxybenzoic acid has been covalently attached to polystyrene-co-divinylbenzene beads at different capacities and the hydroquinone oxidation kinetics have been studied in a stirred batch reactor. An initial rate analysis yielded a first order dependence on the concentration of the substrate hydroquinone and the supported IBX reagent implying chemical reaction is rate limiting. An observed second order rate constant of 1.3 ($\pm$0.3) $M^{-1}\,s^{-1}$ was obtained for the initial rate of oxidation using the supported reagent. The activation energy was halved at later stages of reaction (greater than 50% conversion of the reagent), suggesting that intraparticle diffusion then become rate limiting as the conversion of the reagent in the bead proceeded. Unreacted shrinking core and pseudo-homogeneous diffusion–reaction models have been used to analyse the experimental data to yield values for the effective diffusivity of hydroquinone in the polymer matrix of (1.0–1.2) $\times\ 10^{-11}\ m^2/s$. The performance of the supported reagent in a packed bed has also been studied by continuous flow of a solution of hydroquinone. The product quinone concentration profile at the reactor exit showed limited dependence on the flow-rates studied. Pronounced tailing of the product concentration was obtained for more highly loaded beads, which was attributed to hindered diffusion limiting access to the residual reactive sites.

Keywords: Polymer-supported reagents; IBX; Batch; Packed bed; Model

1. Introduction

Requirements in the pharmaceutical industry for parallel synthesis of libraries of organic compounds has led to the development of simple, high yielding chemical transformations using polymer-supported reagents, scavengers, catalysts and ‘catch and release’ reagents that are amenable to automation. After reactions using insoluble polymer-supported species a simple filtration process allows the product in solution to be recovered with high yield and purity. Recovery of the spent reagent retained on the support allows recycling, thus fulfilling the requirements of environmentally friendly chemistry. The power and elegance of this approach has been demonstrated by Ley and co-workers who recently reported the first fully automated multi-step synthesis of an array of histone deacetylase (HDAc) inhibitors. These were prepared by an unattended reaction sequence incorporating in line ‘catch and release’ purification [1].

The technology presents an exciting potential for manufacturing since the immobilisation and recycling of reagents within a packed or fluidised bed reactor circumvents energy-demanding molecular separation processes and facilitates semi-continuous processing. Consequently equipment sizes, plant inventories and environmental and safety risks can be

* Corresponding author. Tel.: +44 1223 762953; fax: +44 1223 334796.
E-mail address: nkhs2@cam.ac.uk (N.K.H. Slater).

1385-8947/$ – see front matter © 2004 Elsevier B.V. All rights reserved.
doi:10.1016/j.cej.2004.09.004

Nomenclature

C_{A0}	initial concentration of solute in bulk solution (M) (kmol m^{-3})
C_{AB}	concentration of solute in bulk solution (M) (kmol m^{-3})
C_{AS}	concentration of solute at the bead surface (M) (kmol m^{-3})
C_R	concentration of supported reagent (M) (kmol m^{-3})
C_{R0}	initial concentration of immobilised reagent in pellet (M) (kmol m^{-3})
D_B	bulk diffusion coefficient of solute in solution (m^2 s^{-1})
D_e	effective diffusivity of solute in pellet (m^2 s^{-1})
IBX	iodoxybenzoic acid
k_L	liquid side film mass transfer coefficient (m s^{-1})
k_s	pseudo-first order surface reaction rate constant (m s^{-1})
k_V	pseudo-first order reaction rate constant based on volume (s^{-1})
M	mass of polymer-supported reagent (kg)
R	radius of polymer support (m)
r	radial coordinate in the bead (m)
t	time (s)
USC	unreacted shrinking core
V_L	volume of reactor (m^3)
X	conversion of reagent in pellet (–)

Greek symbols

ρ^G	density of the polymer support (kg m^{-3})
τ	dimensionless variable defined in Eq. (9)
ϕ	Thiele modulus defined in Eq. (8)

reduced, so opening the possibility of responsive, local production. In addition the technology overcomes the environmental problems and costs associated with the disposal of spent reagents.

Iodoxybenzoic acid (IBX) is a versatile oxidant [2] for the oxidation of a diverse collection of primary and secondary alcohols. It promotes many other organic transformations including iodinations and epoxidations. We have recently reported the synthesis of polymer-supported IBX by a novel method [3]. The choice of our polymer support material was influenced by a trade-off between capacity, rate of reaction and mechanical stability in stirred reactors and flow through at high pressures in packed beds [4].

Lightly cross-linked polystyrene gels (1–2% DVB) are widely used in polymer assisted solution phase synthesis. These gels swell to many times their original volume in organic solvents and reaction yields are comparable to homogeneous reactions in many cases [5]. Increasing the level of cross-linking enhances the mechanical stability of the polystyrene beads and reduces their swelling ability, leading to a lower solvent volume in the swollen beads. Permanent pores can also be introduced by use of a porogen during the synthesis of the beads, yielding a macroporous structure [4]. Faster rates of conversion of benzyl alcohol to benzaldehyde have been observed for IBX supported on macroporous ‘ArgoPore’ resin as compared with a gel-type ‘Janda’ support [6]. However, the capacities of macroporous beads are generally lower than for gel-type. The mechanical stability of the two resin-types in stirred vessels also differs. In our experience, gel-type resins are generally amenable to use in mechanically stirred reactions that utilise an overhead stirrer and are even relatively stable to short periods of stirring using magnetic stirrers. The more highly cross-linked macroporous resins appear to be less stable when stirred, possibly due to their lower elasticity.

The rate of reactions on the supports can be significantly affected by the ability of reacting species to diffuse through the matrix. In a study of ion exchange processes Helfferich proposed that a model incorporating intrinsic chemical reaction, intraparticle diffusion and interparticle film mass transfer was suitable for analysing mass transfer and reaction in beads [7]. Liberti and Helfferich [8] elaborates on the operating conditions that would enable one of the mass transfer mechanisms to be rate controlling. In a batch reactor, at high solute concentrations and high agitation speeds the intraparticle diffusion in beads could be the rate-limiting step. Conversely, at low solute concentrations and low agitation speeds the external mass transfer may be rate limiting. Few studies have focussed on the scale-up of polymer-supported reactions in reactors based on kinetic measurements. In one study the oxidising reagent Chloramine T supported on Amberlyst 15 resin was used to oxidise S^{2-} in a packed bed [9] and the variation of flow-rate on the breakthrough of reactant was studied. The breakthrough effect was related to the residence time in the reactor, where too high a flow-rate yielded premature breakthrough of S^{2-}.

Furthermore large-scale organic synthesis in packed beds, while promising in practice, has not been pursued aggressively. Overcoming technical difficulties, such as excessive backpressure at high solution flow-rates and swelling of lightly cross-linked beads during chemical reaction, are some of the challenges that need to be overcome. A change in bead swelling brought about by a change in polarity could lead to blockage of packed beds. To counter this monolithic reactors have been developed with polymer beads polymerised within the channels of a porous glass monolith, and the resulting composite used in supporting the reagent [10]. In this work we report on the kinetic characterisation of a polymer-supported IBX reagent and evaluate the performance of a continuous packed bed reactor containing this polymer-immobilised reagent.

2. Experimental

All materials other than functionalised 8% DVB beads were obtained from Sigma–Aldrich and used without further purification. The beads were obtained by suspension polymerisation [4]. The protocol for the synthesis of the support and the subsequent synthesis of the polymer-supported IBX have been reported previously [3].

The pore surface area was obtained from the analysis of N_2 sorption isotherms (Micromeritics ASAP2010). All resin batches were pre-swollen in DMF for 2 h before use to ensure swelling equilibrium was reached. The spherical beads (10 mg) were spread over a glass microscope slide and solvated by adding 1 ml of solvent. The diameter change in a bead was followed with an optical microscope coupled with imaging software. The swelling equilibrium was assumed when there was no further change in particle size. This occurred in 45 min for IBX loaded beads.

The solvent uptake was measured by the centrifugation method [11]. The dry density of the resin was estimated by water displacement. A balance was used to measure the mass of water that was added to make up a total volume of initially dry resin and water of 10 ± 0.005 ml as measured by a micro-volume pipette. The mass of the dry sample was 0.5 ± 0.0002 g and the density of water used was 0.9959 g/ml. This measure yielded the volume of solids and the dry density.

2.1. Reaction monitoring

Spectrophotometric measurements to obtain the concentration of the product benzoquinone in DMF were taken at 360 and 490 nm [12]. This enabled the study of a range of concentrations of benzoquinone. The sample absorbance was stable for up to 30 min when flushed with nitrogen. The Beer Lambert law was followed with an extinction coefficient at 360 nm of 166.4 M^{-1} cm^{-1} and at 490 nm of 14.9 M^{-1} cm^{-1} for the concentration of the quinone product. Continuous monitoring of product formation in the concentration range 1×10^{-5} M to 2×10^{-3} M for batch and 1×10^{-4} M to 1×10^{-1} M for packed bed experiments was thus achieved by following the change in absorbance at 360 and 490 nm, respectively, without the need for dilution.

Fractions collected at regular time intervals were also analysed by gas chromatography to obtain the concentration of hydroquinone and benzoquinone offline. The gas chromatography retention times for solvent, benzoquinone and hydroquinone were 5.4, 11.5 and 22.6 min, respectively, and the difference between the concentrations obtained by spectrophotometry and by gas chromatography for different samples were not significantly different at a 95% confidence level (multiple *t*-test was performed).

2.2. Batch reactor experiments

The batch kinetics were studied in a cylindrical glass vessel (0.5 L capacity) with four internal baffles and a hot water jacket. Ports for sample addition, condenser, stirrer shaft, sample tube, thermocouple and gas inlet for bubbling nitrogen were on a glass lid sealed to the reactor by an O-ring. An overhead stirrer (50–1500 rpm) with a stainless steel shaft and a six-blade rushton turbine (3 cm in diameter for a vessel diameter of 8 cm) was used in all experiments. The sampling tube was made of PTFE with a 0.15 μm PTFE filter connected at one end and placed near the base of the vessel and the other end connected to solvent resistant silicone tubing running through a peristaltic pump and a flowcell in the spectrophotometer and returned to the vessel to ensure a constant reactor volume throughout the reaction. Experiments were conducted with temperature control between 22 and 50 °C (±0.6 °C). A valve was placed between the flowcell and the return to the reactor to enable removal of samples to be periodically analysed offline.

A weighed amount of the free flowing resin was added to the reaction vessel. DMF (80 ml) was then added and the resin was allowed to swell at the required temperature for 2 h. Reactant was added to the vessel in 20 ml of DMF and stirring commenced to initiate the reaction. The entire length of sample tubing initially contained fresh solvent to expel air bubbles that affected the spectrophotometer reading.

2.3. Packed bed experiments

The resin was fed as slurry into a 1-cm × 10-cm glass column fitted with an adapter for varying the column length. The column had chromatographic end fittings to ensure plug flow entry of fluid into the column and end filters to retain the resin. The column was thermostated (±0.6 °C) by a circulating water jacket. Before entry into the column the inlet tubing was immersed in a water bath to preheat the feed. A Pharmacia series P-6000 pump was used to feed the liquid into the column. All solvents used in the packed bed experiments were degassed by connecting to vacuum for 2 h prior to use. With the support material used a constant backpressure and flow-rate was obtained during the reaction. This implied that there was no significant swelling change or irreversible adsorption. The column outlet was connected to a flowcell in the spectrophotometer. Fractions were collected at programmed time intervals and analysed in a GC column.

3. Theoretical development

To model the oxidation reaction several simplifications were made and the utilities of the widely used pseudo-homogeneous diffusion reaction [13] and the unreacted shrinking core models were considered. These models are preferred for their simplicity and the limited number of parameters that need to be independently determined. The simulation of a batch reactor using the two models was compared with the experimentally obtained batch conversion data.

In the unreacted shrinking core (USC) model, a rapid irreversible reaction is considered to occur at the boundary be-

tween an outer shell of spent solid reagent and the unreacted core. In the case of diffusion across the shell being faster than the advance of the moving boundary, a pseudo-steady state assumption is used to yield analytical results. The existence of moving boundaries in reactions involving ion exchange resins was predicted from purely theoretical considerations [14] and has been verified experimentally [15,16]. Furthermore, fluorescence microscopic investigation of the kinetics of polymer-supported reactions has revealed the existence of a shrinking core of unreacted reagent [17] in some cases.

Another possibility is that diffusion and reaction occur simultaneously throughout the resin, and the pseudo-homogeneous diffusion–reaction model is better suited to model this scenario. Using confocal Raman spectroscopy Bradley and coworkers [18] have shown that reaction can occur throughout the bead from an early stage of the reaction.

The unreacted shrinking core model is more applicable to reaction in microporous solids, with greater restriction to solute access. The pseudo-homogeneous model finds application in the modelling of reactions in highly porous solids. Other models of greater complexity have been used in the modelling of liquid phase reactions involving resins. For methyl-*t*-butyl ether (MTBE) synthesis catalysed by macroporous ion exchange resins, a heterogeneous model comprising diffusion and reaction in microspheres, taken as a gel phase, and pore diffusion in macropores situated between these microspheres is used in the modelling of the kinetically controlled reaction [19].

Consider the reaction in the resin. Assume it is isothermal, conducted in dilute solution, and neglect swelling and shrinking during reaction. The following analysis can then be carried out to obtain equations that describe the conversion in the resin.

3.1. Unreacted shrinking core

The unreacted shrinking core approximation yields the rate of concentration change of substrate A in the bulk reactor volume, C_{AB}, whilst undergoing first order reaction with a supported reagent:

$$\frac{dC_{AB}}{dt} = -\frac{3}{R}C_{AB}\left[\left(\frac{1}{k_L}-\frac{R}{D_e}\right)+\frac{R}{D_e}(1-X)^{-1/3}+\frac{1}{k_s}(1-X)^{-2/3}\right]^{-1} \quad (1)$$

where k_L is the film mass transfer coefficient and D_e the intraparticle effective diffusivity of A. X the fractional conversion of the supported reagent and R the support radius. k_s is a pseudo-first order rate constant for the surface reaction and contains the dependence of the intrinsic reaction rate on the initial reagent concentration. The derivation of (1) is given elsewhere [20].

3.2. Pseudo-homogeneous reaction and diffusion model

For the pseudo-homogeneous reaction and diffusion model, Eq. (2) applies for a stoichiometric second order reaction between the substrate and the reagent

$$D_e\left(\frac{\partial^2 C_A}{\partial r^2}+\frac{2}{r}\frac{\partial C_A}{\partial r}\right) = k_V C_A C_{R0}(1-X) \quad (2)$$

where k_V is a rate constant, C_A the concentration of reactant A at depth r in the support, C_{R0} the initial concentration of immobilised reagent and X the fractional conversion at time t. Also:

$$\frac{\partial X}{\partial t} = k_V C_A(1-X) \quad (3)$$

$$\frac{dC_{AS}}{dt} = k_L(C_{AB}-C_{AS}) \quad \text{at } r = R \quad (4)$$

and

$$C_{AB} = C_{A0} \quad (5)$$

$$X = 0 \quad \text{at } t = 0 \quad (6)$$

Ramachandran and Kulkarni [21] derived an approximate solution (7) for the conversion of the resin for this set of equations. The difference between the numerical solution and the approximate solution is less than 17% for a Thiele modulus, φ, of value 10. For the experiments simulated here the Thiele modulus did not exceed 10. As such, the approximate solution was used to simulate the reactor behaviour:

$$\ln\left[\frac{1-X}{0.699}-\frac{\exp(-\tau)}{2.33}\right]+\tau = \frac{\phi^2}{10.5}\times\left[1-\frac{1-X}{0.699}+\frac{\exp(-\tau)}{2.33}\right] \quad (7)$$

where

$$\phi^2 = \frac{k_V C_{R0} R^2}{D_e} \quad (8)$$

$$\tau = k_V C_{AB} t \quad (9)$$

To simulate an isothermal finite volume in a well-stirred batch reactor containing reactant and fully swollen reagent particles, the following design equation applies:

$$C_{R0}\frac{dX}{dt} = \frac{V_L \rho^G}{m}\frac{dC_{AB}}{dt} \quad (10)$$

and for initial conditions (5) and (6),

$$C_{AB} = C_{A0} - \frac{m}{\rho^G V_L}C_{R0}X \quad (11)$$

The ordinary differential equations (1) and (11) were solved for conversion of reagent, X, and concentration of substrate in the bulk solution, C_{AB} using a Runge–Kutta algorithm. While for the pseudo-homogeneous model, the non-linear equations (7) and (11) were solved using the Newton–Raphson method.

Table 1
Properties of the selected functionalised polymer support

Percentage of divinyl benzene (cross-linking)	8	
Particle diameter (dry, μm)	40–150	
Swollen particle diameter (average, μm)	90.4	
Pore diameter distribution (dry, nm)	1.5–2	11–30
Relative pore volume occupied (%)	20	80
Relative surface area (obtained by NLDFT, %)	79	21
Wet bead porosity	0.52	
Dry reagent density (kg/m^3)	1300	
Iodine loading (mmol IBX/g)	3.1	
Active oxidant loading (elemental, mmol IBX/g)	0.2, 0.4, 0.5	
Surface area (BET, m^2/g)	5.1	

4. Results

4.1. Characterisation of the functionalised polystyrene support

In this study an 8% divinyl benzene cross-linked polystyrene resin was used as the support for IBX to reduce swelling variation. The resins were easy to handle and were suitable for packed bed use. The data from N_2 sorption isotherms indicated that the dry functionalised polymer is a gel with a small quantity of accessible micropores. There was evidence of a small quantity of mesopores and macropores in the dry state.

The dry resins had a low internal surface area of 5.1 m^2/g determined from N_2 sorption isotherms utilising the BJH theory [22]. The cumulative pore volume for resins with a pore size less than 480 nm was 0.025 ml/g. The BJH model gave a porosity distribution between 8 and 40 nm, and a mean pore diameter of 19.1 nm. The porosity distribution was also obtained exploiting the non-local density functional theory (NLDFT) model [23]. Utilising this model, the average pore diameter was 1.9 nm in a micropore region contributing to 79% of the cumulative pore surface area. This pore size distribution was well separated from the mesopore to macropore distribution. The larger pore sizes were distributed between 11 and 30 nm with an average pore diameter of 21.4 nm. The relative cumulative volume and the surface area occupied by the separated pore size distributions in the dry state are shown in Table 1.

When swollen in DMF, the equilibrium sorption was 0.8 ± 0.05 g of solvent per gram of dry resin as measured by the centrifugation method. The fraction of solvent volume in the solvent filled polymer gel was calculated as 0.52 ± 0.04. The mean particle size and standard deviation of resin (in hexane) was obtained by dynamic light scattering (Coulter LS230) as 90.4 and 18.3 μm, respectively. The resin had a normal distribution as shown in Fig. 1. The functionalised resins had a dry density of 1.29 ± 0.02 g/ml as measured by water displacement.

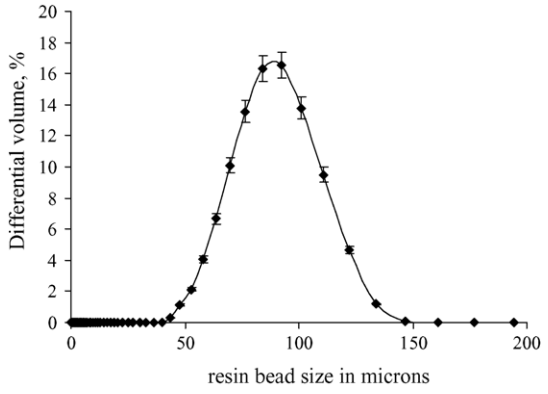

Fig. 1. Resin bead size distribution obtained by light scattering using Coulter LS230. Average pore size of 90.4 μm.

Elemental microanalysis of C, H and I revealed a loading of 3.1 mmol I/g for the iodo-polystyrene, corresponding to 66% of phenyl groups iodinated. Batches of polymer-supported IBX used in this work had loadings of 0.2–0.5 mmol IBX/g by titration with hydroquinone. The oxidation reactions were conducted using DMF as the solvent. The low solubility of hydroquinone in DCM excluded the use of this solvent in the oxidation reaction.

4.2. Experimental batch studies

4.2.1. Effect of stirring speed

The critical impeller speed for complete particle suspension estimated from the Zwittering correlation [24] was 530 rpm for the vessel dimensions and impeller placement. The effect of stirring speed in a batch reactor was studied to elucidate the effect of concentration gradients on the initial rate of reaction. The variation of initial rate [25] with the stirring speed is shown in Fig. 2. Initial rates were obtained from the initial slope in the conversion–time curve. The observed initial rate was independent of stirring speed when the experiment was conducted with a stirring speed greater than 560 rpm. Below this speed the observed initial rate was sig-

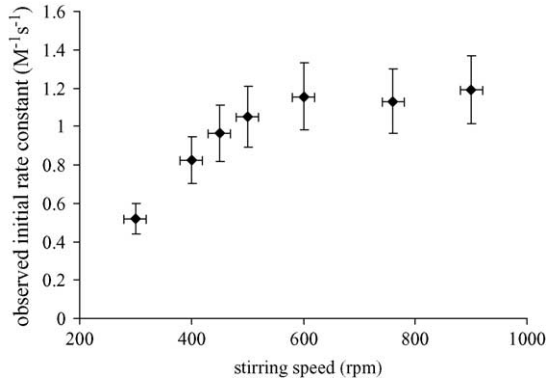

Fig. 2. Effect of stirring speed on the observed initial rate constant of reaction in $M^{-1}\,s^{-1}$ in a baffled 0.5 L stirred tank with overhead stirrer attached to a rushton turbine. The reaction was carried out at 40 °C and between 0.25 g of 0.4 mmol IBX/g and 0.01 M HQ.

nificantly affected by concentration gradients in the reactor. All subsequent reactions were carried out at a stirring speed of 660 rpm. The Frossling correlation [26] yielded an external mass transfer coefficient of 3.6×10^{-4} m/s at this stirring rate.

4.2.2. Effect of concentration

The reaction behaviour at the early stage of conversion of reagent and reactant was studied by calculating the initial rates. The temperature was maintained at 40 °C and all rate constants reported apply to this temperature. The rate dependence on the concentration of hydroquinone was obtained under conditions such that the IBX conversion and the hydroquinone conversion in the reactor did not exceed 30%. Initial rates are plotted against initial hydroquinone concentration in Fig. 3. The method of analysis yields a reaction order of 0.97 (±0.15) for hydroquinone in solution during the early stage of conversion of the resin. Furthermore, the initial reaction rate varied linearly with the mass of polymer-supported IBX reagent used, and more significantly with the loading (or concentration of attached groups). The initial rate was plotted against the active IBX concentration (Fig. 4) in the reactor volume and from this analysis a reaction order of 1.04 (±0.25) was obtained for the concentration of the IBX reagent on the support.

4.2.3. Effect of temperature

The effect of temperature on the conversion of hydroquinone in the range 22–50 °C is shown in Fig. 5. Initial rates were determined from the slopes of these plots and yielded an activation energy of 48 (±4) kJ/mol for 8% DVB polystyrene-supported IBX. During the later stage of reaction, the conversion rapidly decreases and the influence of temperature is less. For conversion of the reagent in this phase the activation energy from the rate data is 28 (±4) kJ/mol (Fig. 6).

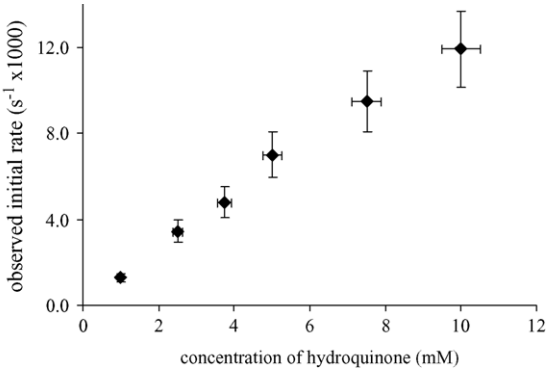

Fig. 3. Initial rate plot for hydroquinone concentration; observed initial rate for concentration of hydroquinone. The observed initial rate shown is in M HQ × M^{-1} IBX × s^{-1} × 1000 and IBX concentration is in mmol of IBX in solvent volume. The rate plot yields an order of 0.97 (±0.07) with respect to hydroquinone from the slope and a rate constant of 1.37 (±0.15) M^{-1} s^{-1} at 40 °C from the gradient.

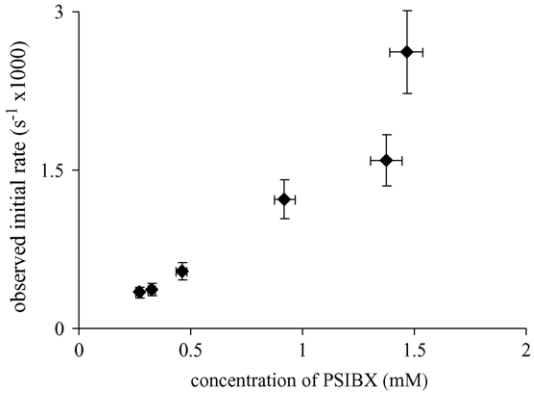

Fig. 4. Initial rate plot for supported IBX concentration; observed initial rate for concentration change of IBX in solvent volume. The observed initial rate shown is in M IBX × M^{-1} HQ × s^{-1} × 1000 and IBX concentration is in mmol of IBX in reactor volume. The rate plot yields an order of 1.04 (±0.13) from the slope and a rate constant of 1.23 (±0.15) M^{-1} s^{-1} at 40 °C from the gradient.

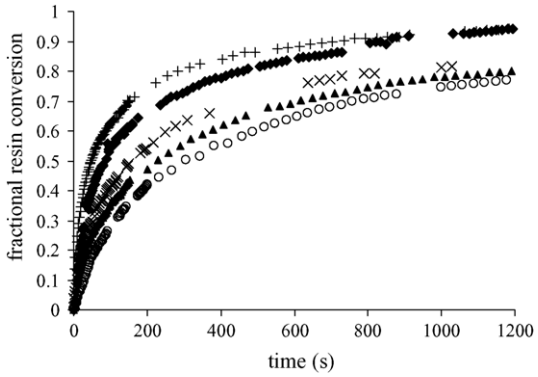

Fig. 5. Conversion–time curves for 0.5 mmol IBX/g resin, reacting with 0.01 M hydroquinone at temperatures of 22.5 °C (◯), 30 °C (▲), 35.5 °C (×), 40 °C (♦), 50 °C (+) in a 100 ml stirred tank operating at 660 rpm.

4.2.4. Intraparticle diffusivity

To determine the intraparticle diffusivity, the experimental batch data were fitted to Eqs. (1) and (7) for the respective models whereby the effective diffusivity parameter was varied to obtain a nonlinear least squares fit to the experimental data for the entire conversion range.

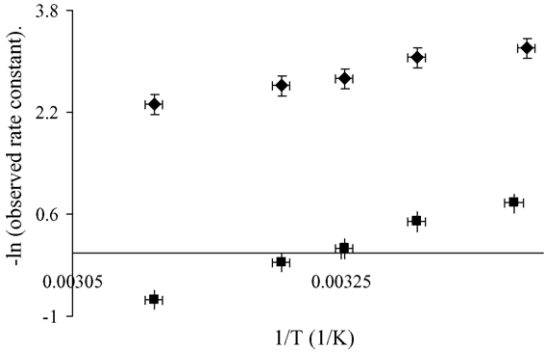

Fig. 6. Activation energy plots for initial rate (■) and later phase (♦) showing the activation energy slope (E_A/R) in chemical reaction rate control and diffusion rate control. Observed rate constant in M^{-1} s^{-1}.

The second order rate constant obtained experimentally from the initial rate analysis was used to obtain an estimate for the intrinsic rate constant for the USC and pseudo-homogeneous reaction models. The heterogeneous analysis using the unreacted shrinking core model uses a pseudo-first order rate constant that incorporates the concentration of the reagent at the reaction interface. This is the initial reagent concentration from the model assumption, which is assumed unchanged within the shrinking core during the course of the reaction. The observed rate constant obtained from the initial rate analysis was also modified to account for the change from a volume to a surface area reference.

For the pseudo-homogeneous model, a single diffusivity parameter could not adequately simulate the conversion over the entire reaction time. For the respective experimental systems shown in Fig. 7, higher diffusivities of 5×10^{-11} m^2/s and 5.5×10^{-11} m^2/s were found to fit the early conversion data selected up to 50% conversion. In the same figures are shown the fits to the conversion throughout the reaction progress, and this corresponds to 1.0×10^{-11} m^2/s and 1.2×10^{-11} m^2/s, respectively, for the 0.2 and 0.4 mmol IBX/g resin loadings. All other experimental conditions, fluid reactant concentration (0.01 M), temperature (40 °C) and stirring speed (660 rpm), were kept constant. The fits obtained using the USC model, Eq. (1), for the experimental runs are shown in Fig. 8. With the USC model, it was possible to identify a single effective diffusivity to fit the entire conversion–time behaviour. Effective diffusivities of 1.0×10^{-11} m^2/s and 1.2×10^{-11} m^2/s were obtained by this method for the 0.2 and 0.4 mmol IBX/g resin.

4.2.5. Packed bed experiments

The flow-rate was varied and the pressure drop per unit length recorded. The data, Fig. 9, show a linear relationship between the pressure drop and the superficial velocity of the fluid phase.

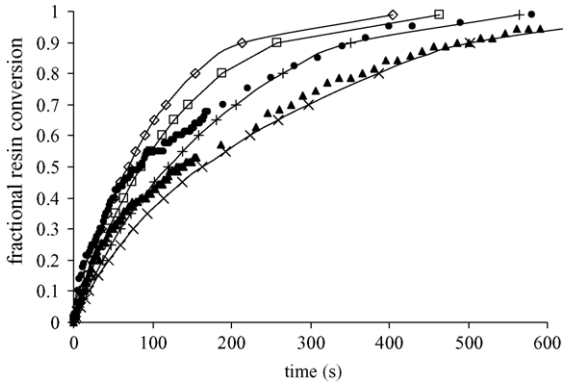

Fig. 7. Conversion–time curves for 0.2 mmol IBX/g (●) and 0.4 mmol IBX/g resin (▲), reacting with 0.01 M hydroquinone at 40 °C in a 100 ml solution stirred at 660 rpm. The pseudo-homogeneous model simulations for effective diffusivities of 5.5×10^{-11} m^2/s (◇ to fit early conversion) and 1.2×10^{-11} m^2/s (□ to fit conversion at end) for 0.2 mmol IBX/g. Simulations with effective diffusivities of 5×10^{-11} m^2/s (+) and 1×10^{-11} m^2/s (×) for 0.4 mmol IBX/g to illustrate the better fit to initial and latter data with different diffusivities.

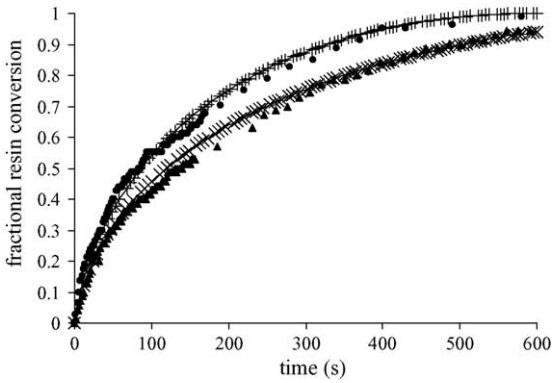

Fig. 8. Conversion–time curves and USC model simulations for 0.2 mmol IBX/g ((●) and (+)) and 0.4 mmol IBX/g resin ((▲) and (×)), reacting with 0.01 M hydroquinone at 40 °C in a 100 ml stirred tank operating at 660 rpm. The effective diffusivity parameter is varied in the simulations, to obtain a diffusivity of 1.2×10^{-11} m^2/s for 0.2 and 1×10^{-11} m^2/s for 0.4 mmol IBX/g.

The flow-rate was also varied for the reaction. The effect of the superficial velocity on the breakthrough profile of the product was observed and is shown in Fig. 10 for a resin loading of 0.5 mmol IBX/g. The fluid volume collected as shown in Fig. 10 is corrected for the dead volume in the column ends, detector and inlet valve from the pump. The fluid reactant feed concentration was increased 10-fold to 0.1 M from the batch study and the temperature was controlled at 40 °C. Also shown is the result for a resin loading of 0.2 mmol IBX/g. A premature breakthrough of product was observed but there is less tailing in the concentration profile than was observed for 0.5 mmol IBX/g.

By integrating the product concentration profile, the loading of the bed was 0.17 (±0.02) mmol IBX/g (0.076 (±0.011) mmol IBX/ml of bed) for the bed with low loading and 0.49 (±0.06) mmol IBX/g (0.21 (±0.02) mmol IBX/ml of bed) for the bed with higher loading.

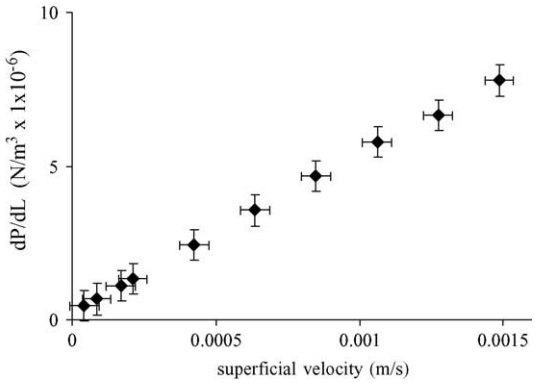

Fig. 9. Influence of mobile phase velocity (m/s) on the pressure drop (N/m^3) across a 4.5 cm long × 1 cm internal diameter packed bed of reagent beads operating at 40 °C.

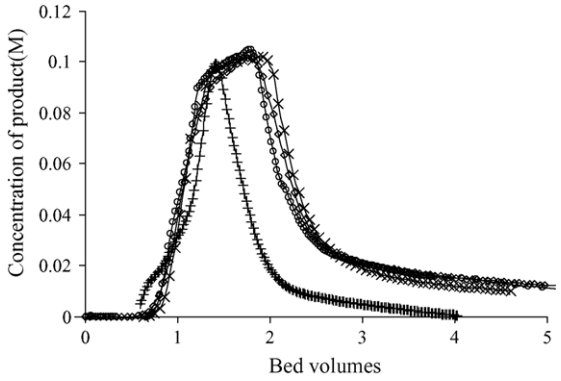

Fig. 10. The product quinone concentration monitored at the exit of the reactor for feed concentration of 0.1 M, bed dimensions 4.5 cm (length) × 1 cm (i.d.) and temperature 40 °C. The bed volume is 3.5 ml for the column dimensions and the resin volume is 2.05 ml. The loading of resin is 0.2 mmol/g and the flow-rate is 0.4 ml/min for (+). The loading is 0.5 mmol/g and the flow-rate is 0.2 ml/min for (◯), 0.4 ml/min for (◊) and 0.8 ml/min for (×).

5. General discussion

The initial rate of reaction follows a first order dependence on both hydroquinone and IBX concentration. This implies that the data has been acquired in the limit of intrinsic chemical reaction control. Santagostino and coworkers [27] observed first order dependence in both reactants in the oxidation of alcohols and 1,2-diols by IBX dissolved in DMF. In that study an inverse dependence on the concentration of water, a by-product of the reaction, was also observed for the reaction.

The intrinsic chemical reaction rate would be expected to vary according to the Arrhenius relationship and in the case of intraparticle diffusion limitation the activation energy of reaction would be expected to halve [28]. The effect of temperature on an external mass transfer controlled reaction would be negligible. This gives a relatively simple means of characterising the different rate-limiting mechanisms during the course of a reaction. An activation energy of 48 ± 4 kJ/mol was found for the initial rate but at a higher conversion of the reagent a much lower activation energy of 28 ± 4 kJ/mol was obtained. The approximate halving of activation energy from the early to the later stages of conversion can be attributed to a change in rate-limiting step from intrinsic chemical reaction to intraparticle diffusion at higher reagent conversion in the resin.

The data analysis has been based on a single effective diffusivity parameter. A model that incorporates a pore diffusion coefficient and a surface or Knudsen diffusion coefficient would adequately describe the longer residence time behaviour in the conversion data. The long tailing might be due to hindered diffusion in micropores of dimensions similar to the molecular size, leading to Knudsen diffusion.

Fig. 1 shows a monodisperse yet broad particle size distribution between 40 and 150 ± 18 μm in diameter. The model uses a single effective diffusivity parameter for this particle size range. For the single diffusivity approach, the USC model is a better fit throughout the course of the reaction.

This study has focused on diffusion as the principal mode of intraparticle mass transfer. Pivonka and Palmer [29] discussed reactant partitioning as a reason for reduced or accelerated reaction rates in supports. The selective uptake or rejection of solute over the solvent can lead to a higher/lower concentration of solute in the resin than in the solution environment. They observed solute partitioning by direct infrared monitoring.

The USC model is based on diffusion rates in the converted 'ash layer' being slower than the reaction rates. Thus chemical reaction rate control at a stage other than for the initial rate is not consistent with the model. In this study, the initial rates were obtained in the limit of chemical reaction control. The shift to diffusion control occurs for higher conversions and the model is thus partially satisfactory. In addition, the more highly loaded resins take longer to fully react, which is consistent with the model.

Jung and coworkers [30] cite adsorption of reactant as contributing to the product gradients they observed using 1% DVB polystyrene resin. They argue that pore diffusion is not rate limiting in the reactions they studied. They obtained a diffusion coefficient of 1×10^{-11} m^2/s (by fitting data of dye elution to a diffusion equation). This is in agreement with the effective diffusivity obtained by our approach for reaction in 8% DVB polystyrene resin. However, they obtained a two orders of magnitude higher diffusion coefficient for small solvent molecules inside the polymer by pulsed field gradient spin-echo NMR. They attribute the difference to fast pore diffusion of solvent molecules and slow surface diffusion of dye molecules after adsorption onto the matrix.

In packed bed conversion, the change in product concentration profile at the reactor exit with volume of effluent is minimal for the different flow velocities studied. The same reagent capacity and length is used in the beds, thus the residence times were different for different flow velocities. Thus residence times in the reactor were adequate for the reactant to be converted in a similar fashion for the different flow velocities studied. The external mass transfer coefficient for a packed bed depends on the mobile phase velocity. For the operating conditions of the packed bed at 0.4 ml/min the mass transfer coefficient is 1.9×10^{-4} m/s, obtained from the correlation of Obashi et al. (see [31]). The external mass transfer rate in the packed bed is much higher than the rate due to the intrinsic chemical reaction for the terms in Eq. (1). This implies that external mass transfer to the resins does not control the kinetics (Table 2).

The rise in product concentration occurs for a volume of fluid that is greater than the bed void volume and less than the total bed volume. The solute is thus taking a tortuous path through the interior of resins at an axial velocity between the superficial and the interstitial velocity in the bed. The use of a lower loading of active reagent on the resin leads to an early fall in conversion at the outlet of the bed as expected.

Table 2
Fixed bed and batch reactor operating conditions

Operating conditions	Batch	Fixed bed
Mobile flow velocity (cm/h)		0.25, 0.51, 1.01
Stirring speed (rpm)	660	
Column dimension (cm)		4.5 (l) × 1 (i.d.)
Temperature (°C)	40	40
Mass of reagent polymer (g)	0.25	1.5
Initial concentration of fluid reactant (mmol/ml)	0.01	0.1
Calculated loading (mmol IBX/g)	0.19[a], 0.36[b]	0.17[a], 0.48[c]

[a] Using PSIBX of active oxidant loading 0.2 mmol IBX/g.
[b] Using PSIBX of active oxidant loading 0.4 mmol IBX/g.
[c] Using PSIBX of active oxidant loading 0.5 mmol IBX/g.

The product breakthrough for the higher loading of reagent on the resin shows a pronounced tailing, and conversion of the reactant continues for a large feed volume. This slow conversion behaviour for the resins is similar to the batch result. This could be attributed to the more highly loaded resins having more of the reagent in less accessible regions in the bead.

The assumptions inherent in the models used to obtain estimates of effective diffusivity are now discussed. For the completely reacted layer to form (the basis of the USC model) the reagent needs to be completely consumed during reaction at the interface. In the case of diffusion being the rate-limiting step for a first order reaction in the concentration of the reagent, a more realistic view is that the reaction is confined to a diffuse region in the pellet as opposed to a sharp interface. The model then applicable is the diffuse interface model [32].

Wen [33] studied the applicability of the pseudo-steady state assumption in the shrinking core model. They concluded that the assumption is valid for liquid–solid reactions when the ratio of the liquid reactant concentration to the resin reagent concentration is less than 0.01. For the loadings of IBX used in this batch study, the ratio is as high as 0.08. This implies that the pseudo-steady state approximation may not be suitable.

The Wilke–Chang correlation [34] was used to predict a bulk diffusion coefficient for hydroquinone in DMF and this was corrected for temperature using the Stokes–Einstein equation relating the temperature, solvent viscosity and diffusion coefficient. A bulk diffusion coefficient of 4.7×10^{-9} m^2/s is obtained at 40 °C. A diffusivity of 4.1×10^{-9} m^2/s was obtained experimentally for benzoquinone product in hexane at 25 °C by Saiki et al. [35]. The much lower effective diffusivity that is predicted from the models could be attributed to Knudsen diffusion in micropores. Low diffusivities of the order of 10^{-11} to 10^{-18} in the polymer gel phase have been used to characterise the sorption and reaction accompanied by diffusion in microporous polystyrene gel-type resins. These values are affected by the diffusion mechanism (pore, Knudsen or surface diffusion). and the polymer architecture. The models are an approximation and the diffusivity parameter while useful, is a result of the model used to obtain it.

6. Conclusions

IBX supported on 8% DVB gel can be easily recovered, and potentially regenerated to be reused. There is, however, experimental evidence of the heterogeneity of the reaction as the reaction proceeds. The reaction rate appears to be chemical reaction controlled at an early stage of conversion of the reagent. However, at the latter stages it appears to be micropore diffusion controlled for the experimental conditions studied. The influence of external mass transfer at the early stage of reaction appears to be small if not negligible. The supported reagent conversion throughout the reaction progress has been modelled as an unreacted shrinking core reaction assuming a pseudo-first order dependence on the fluid phase reactant. A significant influence of intraparticle diffusivity has been observed in the runs on comparing the model to experiment. The pseudo-homogeneous model of reaction and diffusion fits the early conversion well for a higher effective diffusivity than obtained for the shrinking core model, but predicts a shorter time for complete reaction than has been observed experimentally. This model can predict the reaction time by using a smaller diffusivity that is comparable to the values obtained for the USC model of $(1–1.2) \times 10^{-11}$ m^2/s.

Altering the morphology of the support to increase the accessibility to reactive sites could lead to faster kinetics and a more efficient utilisation of the entire reagent quantity supported in the matrix in a particular reaction time. In batch reactions, in driving the fluid phase reactant to full conversion by a near stoichiometric quantity of reagent, the combined effect of low solute concentration and diffusion limitation at higher conversions would lead to the reaction running for prolonged times in order to be taken to completion.

In packed beds, a relatively sharp breakthrough is observed for the product. However, this becomes tailing at high conversion of reagent in the bed. A better utilisation of the available bed capacity is observed for lightly loaded resins in comparison, as this tailing is limited. A longer tail would lead to a poorer bed capacity utilisation, as the product conversion will fall earlier than would be anticipated for the active reagent loading found in batch tests. Thus in order to obtain a pure product, a careful monitoring of the product effluent would be required in this case in order to stop collecting fractions once a threshold in product purity is reached.

References

[1] E. Vickerstaffe, B.H. Warrington, M. Ladlow, S.V. Ley, Org. Biomol. Chem. 1 (14) (2003) 2419–2422.
[2] A. Varvoglis, Hypervalent Iodine in Organic Synthesis, Academic Press, London, 1995.
[3] Z. Lei, C. Denecker, S. Jegasothy, D.C. Sherrington, N.K.H. Slater, A.J. Sutherland, Tetrahedron Lett. 44 (8) (2003) 1635–1637.
[4] D.C. Sherrington, Chem. Commun. 21 (1998) 2275–2286.
[5] S.V. Ley, I.R. Baxendale, R.N. Bream, P.S. Jackson, A.G. Leach, D.A. LongBottom, M. Nesi, J.S. Scott, R.I. Storer, S.J. Taylor, J. Chem. Soc., Perkin Trans. 1 23 (2000) 3815–4195.
[6] N.N. Reed, M. Delgado, C. Hereford, B. Chapman, K.D. Janda, Bioorg. Med. Chem. Lett. 12 (2002) 2047–2049.
[7] F. Helfferich, Ion Exchange, McGraw-Hill, New York, 1962.
[8] L. Liberti, G. Helfferich, Proceedings of the Advanced Study Institute on Mass Transfer and Kinetics of Ion Exchange, Maratea, Nijhoff, Hague, 1982, NATO ASI Ser. E: Appl. Sci. 71 (1982) 193.
[9] E. Kociolek-Balawejder, React. Funct. Polym. 52 (2) (2002) 89–97.
[10] A. Kirschning, C. Altwicker, G. Drager, J. Harders, N. Hoffmann, U. Hoffmann, H. Schonfeld, W. Solodenko, U. Kunz, Angew. Chem. Int. Ed. Engl. 40 (21) (2001) 3995–3996.
[11] D.C. Sherrington, J.A. Greig, Polymer 19 (1978) 163–167.
[12] S. Cao, J. Zhong, K. Hasebe, W. Hu, Anal. Chim. Acta 331 (1996) 257–262.
[13] C.Y. Wen, Ind. Eng. Chem. 60 (9) (1968) 34–42.
[14] F. Helfferich, J. Phys. Chem. 69 (1965) 1178–1185.
[15] P.R. Dana, T.D. Wheelock, Ind. Eng. Chem. Fund. 13 (1974) 20–31.
[16] W.B. Bolden, T. White, F.R. Groves, AIChE J. 35 (5) (1989) 849–852.
[17] R.A. Farrer, G.T. Copeland, M.J.R. Previte, M.M. Okamato, S.J. Miller, J.T. Fourkas, J. Am. Chem. Soc. 124 (9) (2002) 1994–2003.
[18] J. Kress, R. Zanaletti, A. Rose, J.G. Frey, W.S. Brocklesby, M. Ladlow, M. Bradley, J. Comb. Chem. 5 (1) (2003) 28–32.
[19] N.S. Caetano, J.M. Loureiro, A.E. Rodrigues, Chem. Eng. Sci. 49 (24A) (1994) 4589–4604.
[20] O. Levenspiel, Chemical Reaction Engineering, Wiley, London, 1999.
[21] P.A. Ramachandran, B.D. Kulkarni, Ind. Eng. Chem. Process. Des. Develop. 19 (1980) 717–722.
[22] S.J. Gregg, K.S.W. Sing, Adsorption, Surface Area and Porosity, Academic Press, London, 1982.
[23] P.I. Ravikovitch, G.L. Haller, A.V. Neimark, Adv. Colloids Interf. 76–77 (1998) 203–226.
[24] T.N. Zwietering, Chem. Eng. Sci. 8 (1958) 244–263.
[25] S.M. Walas, Reaction Kinetics for Chemical Engineers, Butterworths, 1989, p. 168.
[26] R.H. Perry, D.W. Green, McGraw-Hill, in: Perry's Chemical Engineers' Handbook, 7th ed., 1999, pp. 5–73.
[27] S. Munari, M. Frigerio, M. Santagostino, J. Org. Chem. 61 (1996) 9272–9279.
[28] A. Aris, The Mathematical Theory of Diffusion and Reaction in Permeable Catalysts, vol. 1: The Theory of the Steady State, Clarendon Press, Oxford, 1975, pp. 106–108.
[29] D. Pivonka, D.L. Palmer, J. Comb. Chem. 1 (1999) 294–296.
[30] J. Rademann, M. Barth, R. Brock, H.J. Egelhaaf, G. Jung, Chem. Eur. J. 7 (18) (2001) 3884–3889.
[31] R.H. Perry, D.W. Green, Perry's Chemical Engineers' Handbook, 7th ed., McGraw-Hill, New York, 1999, pp. 2–371.
[32] J.H. Bowen, C.K. Cheng, Chem. Eng. Sci. 24 (1969) 1829–1834.
[33] C.Y. Wen, Ind. Eng. Chem. 60 (1968) 34–39.
[34] C.R. Wilke, P. Chang, Chem. Eng. J. 1 (1955) 264–271.
[35] H. Saiki, K. Takami, T. Toninaga, Phys. Chem. Chem. Phys. 1 (2) (1999) 303–306.